https://doi.org/10.22645/udi.2022.12.15.021
도시과학 제11권 제1호 2022. 12. 21 - 28쪽

Effects of carbonation on hydration characteristics of ordinary Portland cement at pre-curing condition

Kim, Gwang Mok*

Abstract: Raman spectroscopy is effective to investigate functional groups via molecular vibration. The technique offers the structural information of compounds including subtle changes in the chemical composition of local atomic coordination without critical damage. Thus, the effect of carbonation on the hydration characteristics of Portland cement under pre-curing conditions for carbonation was investigated via Raman spectroscopy in the present study. Gaseous CO_2 was injected within 60 seconds, and the reaction time was varied from 0 minute to 90 minutes. The test results indicated that the Ca/Si ratio of C-S-H reduced immediately after mixing and then the C-S-H with a relatively high Ca/Si ratio coexisted as the reaction time increased. The calcium carbonates formed in the present study included calcite and amorphous calcium carbonates. The test results via Raman spectroscopy provide valuable information about the carbonation characteristics of OPC under pre-curing conditions for carbonation.

Key Words: Carbonation, Pre-curing, C-S-H, Hydration characteristics, Ordinary Portland cement

1. Introduction

Referring to Intergovernmental Panel on Climate Change (IPCC), the increase in the global temperature since the mid-20th century is induced by the anthropogenic increase in the concentrations of greenhouse gas (Florides and Christodoulides, 2009). Carbon dioxide is one of the representative greenhouse gases. The CO_2 including water vapour, methane, and so on traps outgoing infrared radiation, leading to a temperature increase (Florides and Christodoulides, 2009). The phenomenon is called the greenhouse effect (Zhong and Haigh, 2013).

The cement industry is one of the major contributors to emitting CO_2 (Mehta, 2002). A large amount of CO_2 in the manufacturing process of cements is released. The CO_2 emission as each ton of cement production is reportedly one tonne, which is mostly generated by the de-carbonation of limestone and consumption of fossil fuel (Worrell et al., 2001). The total emission of CO_2 in the cement industry is approximately 5 % of global CO_2 emissions (Worrell et al., 2001).

Therefore, various techniques including blended cements utilizing industrial byproducts, carbonation curing, and alternative binder synthesis to reduce CO_2 emission in the cement industry were proposed (Herath et al., 2020; Zhang et al., 2017; Rungchet et al., 2017). The blended cements employ industrial byproducts such as fly ash and blast furnace slag which slowly react due to pozzolanic reaction (Zhang et al., 2000). The type of cement can contribute to the reduction in CO_2 emission from the use of cements since the use of Portland cements can be reduced (Nath and Sarker, 2011). The synthesis of alternative cementitious materials utilizing byproducts can reduce CO_2 emission since the temperature for the synthesis is lower than that for the manufacturing of Portland cements. For example, the calcination temperature of calcium sulfoaluminate cements was reportedly $\approx$1,250 °C, while that of ordinary portland cement was 1,500 °C (Tan et al., 2020). Furthermore, the use of limestone can be reduced by utilizing Ca-rich byproducts.

Carbonation curing is the technique in which Ca components leached from Ordinary portland cement powder during hydration reacts with CO_2 and forms calcium carbonates (Zhang and Shao, 2016). That is, CO_2 is mineralized during this process (McConnell et al., 2017). The technique was proposed in the 1970s (Zhang et al., 2017). However, studies on the technique

* 한국지질자원연구원 광물자원연구본부 선임연구원, 교신저자 (k.gm@kigam.re.kr).

were not actively conducted at that time, as the carbonation that occurred in cementitious matrix was considered negative effect on the durability of concrete (Zhang et al., 2017).

Recently, studies on the carbonation curing of cementitious materials actively conducted. In general, carbonation curing is divided into two stages. Pre-curing (first stage) is initiated before casting. CO_2 exposure begins immediately after cement powders come into contact with water. The carbonation process terminates within tens of seconds (Shi et al., 2012). Pre-curing is applicable in the production process of ready-mixed concrete. The second stage is "CO_2 exposure" in which CO_2 sources are provided for a few days (Kashef-Haghighi and Ghoshal, 2010), after casting for a few hours and demolding. Gaseous CO_2 is generally used in the stage, but supercritical CO_2 has been used in some studies (Fernández-Carrasco et al., 2008). The second stage is applicable in the production process of precast concretes.

In particular, the investigation of the reaction characteristics of Portland cements under pre-curing condition is critical, since the leached calcium components from cement powders enable them to competitively form hydrates or calcium carbonates. That is, carbonation under pre-curing condition could significantly affect the structural characteristics of hydrates, which determine the mechanical properties and durability of cementitious materials.

Thus, the effect of carbonation on the hydration characteristics of Portland cement under pre-curing condition was investigated via Raman spectroscopy in the present study. Gaseous CO_2 was injected within 60 seconds, and the reaction time was varied from 1 minute to 90 minutes.

2. Experimental Procedure

2.1 Raw materials

The binder material used in the present study was Ordinary Portland cement (OPC), and the chemical composition was shown in Table 1. The CO_2 for the carbonation of OPC powder was supplied in a gaseous state. Anhydrous ethanol (guaranteed reagent grade, OCI Company Ltd.) was used to prevent an additional reaction.

Table 1. Chemical composition of OPC

Components	Composition (%)
CaO	65.5
SiO_2	17.9
Al_2O_3	4.75
Fe_2O_3	3.67
SO_3	3.31
MgO	2.6

2.2 Sample preparation and test methods

The schematic diagram of the experimental setup for the carbonation of OPC powder in pre-curing condition was shown in Fig. 1.

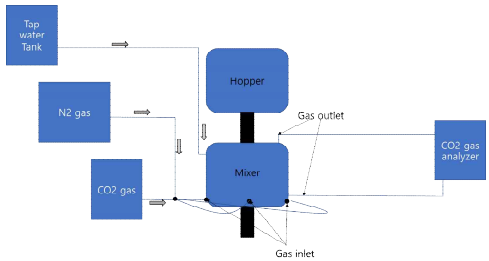

Fig. 1. Schematics of experimental setup for carbonation of OPC powder in pre-curing conditioin

The setup was composed of CO_2, N_2, and tap water tank, a sealed mixer, and a CO_2 gas analyzer. N_2 was used as a purging gas to remove atmospheric CO_2 gas. The concentration of the atmospheric CO_2 gas during purging was measured with a CO_2 gas analyzer. The Mixer used here was sealed with a closed box to minimize leakage of injected CO_2 gas during mixing and to prevent the reaction of atmospheric CO_2. The mixing procedure was as follows: The OPC powder was added to the mixer, and the sealing box was closed. The N_2 gas was introduced to remove atmospheric CO_2. Tap water was then injected into the mixer and mixing was conducted simultaneously. The water to cement ratio was fixed at 0.4. The mixing was maintained for 30 seconds and CO_2 gas was afterward introduced for 60 seconds. Then, the mixture was filled in centrifuge tubes of 60 ml and sealed. Anhydrous ethanol was poured into the tubes to arrest additional reaction after

the designated reaction periods.

Raman spectroscopy (LabRAM HR Evolution Visible_NIR, Horiba) in the present study was used to investigate the structural characteristics of hydrates induced by the carbonation at pre-curing condition. The technique is effective to investigate functional groups via molecular vibration (Wilson et al., 1980). The technique offers the structural information of compounds including subtle changes in the chemical composition of local atomic coordination without critical damage (Kavetskyy et al., 2007). Furthermore, additional sample treatment steps are not required. The excitation source was fixed at 633 nm, and the spectral range was from 500 cm^{-1} to 1600 cm^{-1}. The corresponding values of the grating, visible range, and acquisition time were 600 line/min, 500 nm, and 60 seconds. A 50× objective with long working distance was used for samples.

3. Results and Discussion

Figure 2 shows Raman spectra of OPC powders carbonated under pre-curing condition, and table 2 shows the summary of peaks assigned to the spectra in the present study. Here, C0 represents the powder sample obtained from mixture immediately after mixing for 1 minute, while C90 represents the powder sample additionally reacted for 90 minutes after mixing.

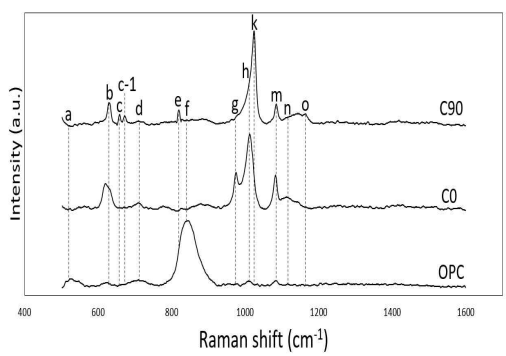

Fig 2. Representative Raman spectra of OPC powder carbonated under pre-curing condition

The peak observed at about 500 cm^{-1} (peak a) in the spectrum of pristine OPC sample is assigned to the $\nu 1$ symmetric stretching of Al-O in AlO_4^{5-} units which is attributed to calcium aluminate phases in clinker (Garg et al., 2013). The calcium aluminate phase in OPC powder is generally C_3A which is rapidly dissolved when contacting with water (Garg et al., 2013). The broadband in the frequency range of 780 cm^{-1} – 920 cm^{-1} (peak f) in the OPC powder sample is assigned to alite and belite phases which are common clinker phases (Mohaček-Grošev et al., 2021). The peak was significantly diminished as the reaction time increased, indicating that the clinker phases are rapidly dissolved upon contact with water.

The peak observed at about 625 cm^{-1} (peak b) of C0 and C90 spectra is attributed to the outer layer of C-S-H gel which could be observed at a very early age of curing of OPC (Taylor, 1997). Liu et al. reported that the outer layer of C-S-H gel surrounded cement grains at a very early age of curing (Liu et al., 2015). The peak b observed in C0 Spectrum indicated that the outer layer of C-S-H gel in the present study was formed immediately after mixing. The peak in the present study was more clear compared to that in the previous studies. It has been reported in previous studies that the outer layer of C-S-H gel could not be observed after the sufficient evolution of C-S-H phases (Sun et al., 2021; Taylor, 1997). That is, the evolution of the C-S-H phase under pre-curing condition was possibly hindered.

The peaks observed at about 660 cm^{-1} (peak c) and 670 cm^{-1} (peak c-1) in the C90 spectrum are assigned to Q^2 Si-O-Si symmetric bending vibration and are attributed to the presence of C-S-H phases (Tang et al., 2021). The peak assigned to Q^2 Si-O-Si symmetric bending vibration in hydrated OPC powder was reportedly observed at about 670 cm^{-1} (Tang et al., 2021). The peak c could be shifted to a lower frequency as the Ca/Si ratio in C-S-H decreased (Garbev et al., 2007; Tang et al., 2021). Tang et al. reported that the peak could be shifted to 660 cm^{-1} when carbonation of the C-S-H phase occurred (Tang et al., 2021). That is, a part of C-S-H phases with lower Ca/Si ratio due to the carbonation under pre-curing condition coexisted with those with relatively high Ca/Si ratio. While, the peaks were not

clearly observed in the C0 spectrum, indicating that the carbonation under pre-curing condition dominantly occurred during mixing.

Table 2. Summary of peaks assigned to the spectra in the present study

Peak	Frequency (cm^{-1})	Assignment	References
a	~500	v1 symmetric stretching of Al-O in AlO_4^{5-} units	Garg et al., 2013
b	625	outer products of C-S-H	Taylor, 1997
c	660	Q^2 Si-O-Si symmetric bending vibration (decalcification of C-S-H)	Tang et al., 2021
d	670	v4 in-plane bending vibration of C-O in CO_3^{2-} units	Garbevet al., 2007
e	825	Q^0 symmertric stretching vibration in Si-O-Si	Ortaboy et al., 2017
f	780-920	alite and belite phases	Garg et al., 2013
g	976	Q^1 asymmetric stretching of Si-O-Si	Tang et al., 2021
h	1015	antisymmetric stretching vibration of S-O in SO_4^{2-} units	Potgieter-Vermaak et al., 2006
		v3 symmetric stretching of Q^2 in Si-O-H or Si-O-Ca	Zhu et al., 2020
k	1024	v1 symmetric stretching of S-O SO_4^{2-} units	Torres-Carrasco et l., 2017)
m	~1088	v1 symmetric stretching of C-O in CO_3^{2-} units	Gabrielli et al., 2000
n	1130	ν6-type deformation mode of Si-O-Si linkage	McMillan, 1984
o	1160	ν9-type deformation mode of Q^4	Kihara et al, 2005

The peak observed at about 825 cm^{-1} (peak e) of the C90 spectrum is attributable to the presence of a residual silicate source which was not consumed when forming hydrates (Ortaboy et al., 2017). The peak is assigned to the Q^0 symmetric stretching vibration (Ortaboy et al., 2017). That is, SiO_2 components were possibly left behind drying process of C90 samples. It can be inferred from the result that partial Si components leached from OPC powder under pre-curing condition did not participate in the formation of the C-S-H phase, since a part of Ca components leached from OPC powder were consumed by forming calcium carbonates (He et al., 2021).

The peak observed at about 976 cm^{-1} (peak g) in the C0 spectrum is assigned to the Q^1 asymmetric stretching vibration of Si-O-Si, which indicates the presence of the C-S-H phase. The peak g in the C90 spectrum was significantly diminished, which could be reportedly led by the decalcification of the C-S-H phase (Tang et al., 2021).

It was reported in the previous studies that the peak observed at 1010 cm^{-1} was induced by the symmetric stretching vibration of SO_4^{2-} units, and the peak was shifted to 1015 cm^{-1} due to the formation of ettringite (Potgieter-Vermaak et al., 2006; Bensted, 1977). That is, the peak observed at about 1015 cm^{-1} (peak h) in the C0 spectrum indicated the formation of ettringite immediately after mixing. The peak h in the C0 spectrum was diminished in the C90 spectrum, while the peak at about 1024 cm^{-1} (peak k) was newly observed in the C90 spectrum. The peak k is assigned to the symmetric stretching vibration of SO_4^{2-} and is attributed to the presence of gypsum (Buzatu et al., 2016). Bensted reported that a partial ettringite phase could be decomposed due to a carbonation reaction (Bensted, 1977). The decomposition of ettringite due to carbonation under pre-curing condition was probably responsible for the reduction in the intensity of peak h, and the clear occurrence of peak k. Meanwhile, the peak h could be also assigned to the $\nu 3$ symmetric stretching of Q^2 in Si-O-H or Si-O-Ca (Torres-Carrasco et al., 2019). In general, the peak h has been clearly observed in the previous studies on the characterization of synthesized C-S-H via Raman spectroscopy (Ortaboy et al., 2017; Tang et al., 2021). Tang et al. reported that the intensity of peak h increased as carbonation progressed, indicating that silicate units were

more polymerized. Despite of that it was difficult to distinguish the symmetric stretching vibration of SO_4^{2-} and $\nu 3$ symmetric stretching of Q^2 in Si-O-H or Si-O-Ca in the present study, it seems that the attenuation of the peak h was mostly induced by the carbonation of ettringite under pre-curing condition. The peak assigned to $\nu 3$ symmetric stretching vibration of Q^2 in Si-O-H or Si-O-Ca was not generally clear in hydrated OPC (Wang et al., 2022).

The peak observed at about 1088 cm^{-1} (peak m) in the C0 spectrum is assigned to $\nu 1$ symmetric stretching vibration of C-O in CO_3^{2-} units due to the presence of calcite (De La Pierre et al., 2014). The peak m (~ 1084 cm^{-1}) in the C0 spectrum was shifted to low frequency compared to that in the OPC spectrum. It has been reported that Si and Mg components could offer stability to ACC during the formation of calcium carbonates since the presence of Mg and Si led to the positional disordered of CO_3^{2-} ions (Fu et al., 2014; Wang et al., 2012). The dissolution of OPC powder introduces the Si and Mg components in the mixture. That is, the shift of peak m indicated that calcium carbonates formed in the C0 sample were more disordered due to the presence of Si and Mg leached from OPC powder. Furthermore, the weak peak observed at about 714 cm^{-1} (peak d) in the C0 spectrum is assigned to $\nu 4$ in-plane bending vibration of C-O in CO_3^{2-} units, indicating the presence of amorphous calcium carbonates (ACC) (De La Pierre et al., 2014) That is, the results indicated that ACC under pre-curing condition was formed immediately after mixing (Wang et al., 2012). Meanwhile, the peak m in the C0 spectrum was shifted to high frequency (~ 1086 cm^{-1}) in the C90 spectrum. Furthermore, the peak d in the C90 spectrum was diminished. The results indicated that ACC formed in the C0 sample was transformed into calcite phases. It is well known that the ACC phase is unstable and readily transformed into calcium carbonate polymorphs (Fu et al., 2014).

The peaks observed at about 1130 cm^{-1} (peak n) and 1160 cm^{-1} in the C0 and C90 spectra (peak o) are assigned to the $\nu 6$-type deformation mode of O atoms in Si-O-Si units and $\nu 9$-type deformation mode of Q^4, respectively. The peaks indicated the presence of C-S-H. Ortaboy et al. reported that the intensity of the peak n increased as the Ca content in C-S-H increased (Ortaboy et al. 2017). The peak n in the C90 spectrum was reduced compared to that in the C0 spectrum. The results indicated that the Ca/Si ratio of C-S-H under pre-curing condition decreased as the reaction time increased. Meanwhile, the intensity of peak o in the C90 spectrum increased compared to that in the C0 spectrum. The increase in the intensity of the peak o could be induced by further polymerization of the silicate chain. However, a further study is needed. As aforementioned, the evolution of C-S-H in the present study was quite complicated as increasing reaction time, since the supply of CO_2 was cut off within mixing time. The formation of C-S-H phases was favored after cutting off the CO_2 injection since the injected CO_2 was quickly consumed by the carbonation reaction.

4. Concluding remarks

The effect of carbonation on the hydration characteristics of Portland cement under pre-curing condition was investigated via Raman spectroscopy in the present study. The test results indicated that the carbonation reaction dominantly occurred immediately during mixing. The reaction products were disordered calcite and ACC. Then, the crystallinity of calcite was improved and ACC was not detected as the reaction time increased. The ettringite phase was also immediately formed upon contacting water and was transformed into gypsum in the C90 sample due to the carbonation of the ettringite. For the C-S-H phase, the outer layer C-S-H phase was rapidly formed and the structural characteristics were affected under pre-curing condition. In detail, the Ca/Si ratio of the C-S-H phase in the C0 sample was reduced by the decalcification of the Q^1 site in the phase. The structural characteristics of the C-S-H phase in the C90 sample were more complicated due to the formation of additional C-S-H under the conditions that the CO_2 supply was cut off.

감사의 글

This work was supported by Korea Institute of Energy Technology Evaluation and Planning(KETEP) grant funded by the Korea government(MOTIE)(20212010200080, In-situ carbonation technology development using CO_2 emissions from cement industry).

REFERENCES

Buzatu, A., Dill, H. G., Buzgar, N., Damian, G., Maftei, A. E., Apopei, A. I. (2016), "Efflorescent sulfates from Baia Sprie mining area (Romania)—acid mine drainage and climatological approach." Science of the Total Environment, Vol. 542, pp. 629-641.

De La Pierre, M., Carteret, C., Maschio, L., André, E., Orlando, R., Dovesi, R. (2014), "The Raman spectrum of $CaCO_3$ polymorphs calcite and aragonite: a combined experimental and computational study." The Journal of Chemical Physics, Vol. 140(16), pp. 164509.

Fernández-Carrasco, L., Rius, J., Miravitlles, C. (2008), "Supercritical carbonation of calcium aluminate cement." Cement and concrete research, Vol. 38(8-9), pp. 1033-1037.

Florides, G. A., Christodoulides, P. (2009), "Global warming and carbon dioxide through sciences." Environment international, Vol. 35(2), pp. 390-401.

Fu, F., Tian, L. G., Xu, S., Xu, X. G., Hu, X. B. (2014), "Synthesis of stable ACC using mesoporous silica gel as a support." Nanoscale Research Letters, Vol. 9(1), pp. 1-6.

Gabrielli, C., Jaouhari, R., Joiret, S., Maurin, G. (2000), "In situ Raman spectroscopy applied to electrochemical scaling. Determination of the structure of vaterite." Journal of Raman Spectroscopy, Vol. 31(6), pp. 497-501.

Garbev, K., Stemmermann, P., Black, L., Breen, C., Yarwood, J., Gasharova, B. (2007), "Structural features of C-S-H (I) and its carbonation in air—a Raman spectroscopic study. Part I: fresh phases." Journal of the American Ceramic Society, Vol. 90(3), pp. 900-907.

Garg, N., Wang, K., Martin, S. W. (2013), "A Raman spectroscopic study of the evolution of sulfates and hydroxides in cement-fly ash pastes." Cement and Concrete Research, Vol. 53, pp. 91-103.

He, R., Zhang, S., Zhang, X., Zhang, Z., Zhao, Y., Ding, H. (2021), "Copper slag: The leaching behavior of heavy metals and its applicability as a supplementary cementitious material." Journal of Environmental Chemical Engineering, Vol. 9(2), pp. 105132.

Herath, C., Gunasekara, C., Law, D. W., Setunge, S. (2020), "Performance of high volume fly ash concrete incorporating additives: A systematic literature review." Construction and Building Materials, Vol. 258, pp. 120606.

Kavetskyy, T., Vakiv, M., Shpotyuk, O. (2007), "Charged defects in chalcogenide vitreous semiconductors studied with combined Raman scattering and PALS methods." Radiation Measurements, Vol. 42(4-5), pp. 712-714.

Kashef-Haghighi, S., Ghoshal, S. (2010), "CO_2 sequestration in concrete through accelerated carbonation curing in a flow-through reactor." Industrial & engineering chemistry research, Vol. 49(3), pp. 1143-1149.

Kihara, K., Hirose, T., Shinoda, K. (2005), "Raman spectra, normal modes and disorder in monoclinic tridymite and its higher temperature orthorhombic modification." Journal of Mineralogical and Petrological Sciences, Vol. 100(3), pp. 91-103.

Liu, F., Sun, Z., Qi, C. (2015), "Raman spectroscopy study on the hydration behaviors of Portland cement pastes during setting." Journal of Materials in Civil Engineering, Vol. 27(8), pp. 04014223.

McConnell, J., Stone, E. N., PE, E., Yost, J. R., Sustainability, S. E. I., Bridge, S. (2017), "Optimizing Concrete for More Sustainable Bridges" STRUCTURE, Vol. 19.

McMillan, P. (1984), "Structural studies of silicate glasses and melts—applications and limitations of Raman spectroscopy." American Mineralogist, Vol. 69(7-8), pp. 622-644.

Mehta, P. K. (2002), "Greening of the concrete industry for sustainable development." Concrete international, Vol. 24(7), pp. 23-28.

Mohaček-Grošev, V., Đuroković, M., Maksimović, A. (2021), "Combining raman spectroscopy, dft calculations, and atomic force microscopy in the study of clinker materials." Materials, Vol. 14(13), pp. 3648.

Nath, P., Sarker, P. (2011), "Effect of fly ash on the durability properties of high strength concrete." Procedia Engineering, Vol. 14, pp. 1149-1156.

Ortaboy, S., Li, J., Geng, G., Myers, R. J., Monteiro, P. J., Maboudian, R., Carraro, C. (2017), "Effects of CO_2 and temperature on the structure and chemistry of C-(A)-S-H investigated by Raman spectroscopy." RSC advances, Vol. 7(77), pp. 48925-48933.

Potgieter-Vermaak, S. S., Potgieter, J. H., Van Grieken, R. (2006), "The application of Raman spectrometry to investigate and characterize cement, Part I: A review." Cement and concrete research, Vol. 36(4), pp. 656-662.

Rungchet, A., Poon, C. S., Chindaprasirt, P., Pimraksa, K. (2017), "Synthesis of low-temperature calcium sulfoaluminate -belite cements from industrial wastes and their hydration: Comparative studies between lignite fly ash and bottom ash." Cement and Concrete Composites, Vol. 83, pp. 10-19.

Shi, C., He, F., Wu, Y. (2012), "Effect of pre-conditioning on CO_2 curing of lightweight concrete blocks mixtures." Construction and Building materials, Vol. 26(1), pp. 257-267.

Sun, H., Zhang, X., Zhao, P., Liu, D. (2021), "Effects of Nano-Silica Particle Size on Fresh State Properties of Cement Paste." KSCE Journal of Civil Engineering, Vol. 25(7), pp. 2555-2566.

Tan, B., Okoronkwo, M. U., Kumar, A., Ma, H. (2020), "Durability of calcium sulfoaluminate cement concrete." Journal of Zhejiang University-SCIENCE A, Vol. 21(2), pp. 118-128.

Tang, C., Ling, T. C., Mo, K. H. (2021), "Raman spectroscopy as a tool to understand the mechanism of concrete durability—a review." Construction and Building Materials, Vol. 268, pp. 121079.

Taylor, H. F. (1997), "Cement chemistry" Vol. 2, pp. 459. London: Thomas Telford.

Torres-Carrasco, M., del Campo, A., de la Rubia, M. A., Reyes, E., Moragues, A., Fernández, J. F. (2017), "New insights in weathering analysis of anhydrous cements by using high spectral and spatial resolution Confocal Raman Microscopy." Cement and Concrete Research, Vol. 100, pp. 119-128.

Wang, D., Hamm, L. M., Bodnar, R. J., Dove, P. M. (2012), "Raman spectroscopic characterization of the magnesium content in amorphous calcium carbonates." Journal of Raman Spectroscopy, Vol. 43(4), pp. 543-548.

Wang, Z., Chen, Y., Xu, L., Zhu, Z., Zhou, Y., Pan, F., Wu, K. (2022), "Insight into the local CSH structure and its evolution mechanism controlled by curing regime and Ca/Si ratio." Construction and Building Materials, Vol. 333, pp. 127388.

Wilson, E. B., Decius, J. C., Cross, P. C. (1980), "Molecular vibrations: the theory of infrared and Raman vibrational spectra." Courier Corporation.

Worrell, E., Price, L., Martin, N., Hendriks, C., Meida, L. O. (2001), "Carbon dioxide emissions from the global cement industry." Annual review of energy and the environment, Vol. 26(1), pp. 303-329.

Zhang, D., Shao, Y. (2016), "Early age carbonation curing for precast reinforced concretes." Construction and Building Materials, Vol. 113, pp. 134-143.

Zhang, D., Ghouleh, Z., Shao, Y. (2017), "Review on carbonation curing of cement-based materials." Journal of CO_2 Utilization, Vol. 21, pp. 119-131.

Zhang, Y. M., Sun, W., Yan, H. D. (2000), "Hydration of high-volume fly ash cement pastes." Cement and Concrete Composites, Vol. 22(6), pp. 445-452.

Zhong, W., Haigh, J. D. (2013), "The

greenhouse effect and carbon dioxide." Weather, Vol. 68(4), pp. 100-105.

Zhu, X., Zhang, M., Yang, K., Yu, L., Yang, C. (2020), "Setting behaviours and early-age microstructures of alkali-activated ground granulated blast furnace slag (GGBS) from different regions in China." Cement and Concrete Composites, Vol. 114, pp. 103782.